Theoretical and Experimental Study on a Self-Assembling Polysaccharide Forming Nanochannels: Static and Dynamic Effects Induced by a *Soft* Confinement

Gianfranco Bocchinfuso,[†] Antonio Palleschi,*[,†] Claudia Mazzuca,[†] Tommasina Coviello,[‡] Franco Alhaique,[‡] and Giovanni Marletta[§]

Dipartimento di Scienze e Tecnologie Chimiche, University of Roma "Tor Vergata", via della Ricerca Scientifica, 00133 Roma, Italy, Dipartimento di Studi di Chimica e Tecnologia delle Sostanze Biologicamente Attive, Università di Roma "La Sapienza", P.le Aldo Moro 5, 00185 Roma, Italy, and Dipartimento di Scienze Chimiche, Università di Catania, viale A. Doria, 95125 Catania, Italy

Received: July 31, 2007; Revised Manuscript Received: December 28, 2007

It is well-known that the polysaccharide scleroglucan (Sclg) exhibits a triple-helix conformation (triplex) and it is able to form hydrogels in water solution. Furthermore, these hydrogels are influenced by the presence of borax, in terms of rheological and drug release properties. In previous works, we showed that the presence of borax stabilizes the intertriplex interactions and that the property variations, induced by borax, can be fully explained, considering that the Sclg triplexes can form nanochannel-like structures. In this paper, the stability of these aggregates has been experimentally studied by means of atomic force microscopy (AFM) and theoretically investigated by means of molecular dynamics (MD) simulations. The simulations indicate that the borax stabilizes nanochannel-like structures when seven triplexes are considered. The simultaneous presence of different Sclg triplexes in a narrow space strongly influences the properties of confined water molecules in a way similar, in many aspects, to that of water molecules located in the inner part of well-defined nanochannels (e.g., diffusion inside carbon nanotubes). As a consequence, also the conformational properties of flanking regions of Sclg triplexes are influenced. Furthermore, differential scanning calorimetry (DSC) data show that the well-known conformational transition occurring at 280 K for Sclg does not take place in the presence of borax. The MD simulations suggest that such lack of transition is a direct consequence of the presence of borax. The role of Na^+ counterions in the hydrogel structure is also investigated.

1. Introduction

Scleroglucan (Sclg), a polysaccharide secreted by fungi of the genus *Sclerotium*, exhibits a backbone build up by (1 → 3) linked β-D-glcp units with single glc *p* side chains linked β-(1 → 6) to every third residue in the main chain (Figure 1). Sclg has been successfully used for various applications (secondary oil recovery, ceramic glazes, food, paints, cosmetics, etc.).[1] From a structural point of view Sclg exhibits a triple-helix conformation (Triplex) (Figure 2) both in aqueous solution[2] and in the solid state (fiber analyses[3]). These data lack atomistic details but give evidence that the triplex is sustained by a network of interchain H-bonds among the hydroxyl groups linked to the C-2 atoms of the glucose units of the backbone. It is well-known that three-dimensional details of saccharides are difficult to obtain experimentally, because many molecules do not crystallize and their NMR signals are highly overlapped; frequently, the spectra contain second-order line-shape resonances.[4] It is, therefore, usual to use computational techniques to complement experimental data in order to obtain structural information. We have shown by means of molecular dynamics (MD) simulations of a triplex in water that the H-bond network described above is strongly retained in aqueous solution, confirming its importance for triplex stability and properties, in particular for its high stiffness,[5] as recently confirmed by Kony et al.[6] Furthermore, we described the effect of triplex superstructures both on the surrounding water molecules and on the mobility of the side-chain glucose rings at different temperatures. These two aspects appear to be determinant for the characterization of the conformational cooperative transition, experimentally observed at about 280 K by means of optical rotation, heat capacity, viscosity,[7,8] NMR,[9] and dielectric dispersion.[10] In fact, this transition is thought to depend on the mobility of the side chains (side-glcps, D-rings in Figure 1) mediated by the first shells of hydration water molecules.[11] In particular, we showed that some water molecules surrounding the triplex are significantly influenced by temperature and could play a crucial role in the aforementioned transition.

With the aim of obtaining a molecular system suitable for sustained drug release formulations, we have previously described the effects on Sclg gelation of the presence of borax (Sclg/borax), which has the ability to cross-link polymers with hydroxyl groups.[12–15] In particular, we showed that a mixed chemical/physical linkage takes place and that the intermolecular cross-links are essentially of physical nature.[13]

At the same time, a surprisingly noticeable anisotropic swelling behavior of tablets obtained from the freeze-dried hydrogel has been described.[14] Recently, we reported an MD investigation of the influence of the borax groups on the intertriplex interaction:[16] two triplexes have been simulated in water solution with and without borax. Only in the simulation with borax was the starting configuration, with the axes of the two triplexes parallel, retained. Starting from these data, we supposed that, in the presence of borax, groups of Sclg triplexes aggregate

* To whom correspondence should be addressed. Tel.: 0039-06-72594466. Fax: 0039-06-72594328. E-mail: antonio.palleschi@uniroma2.it.
† University of Roma "Tor Vergata".
‡ Università di Roma "La Sapienza".
§ Università di Catania.

10.1021/jp076074f CCC: $40.75
Published on Web 04/17/2008

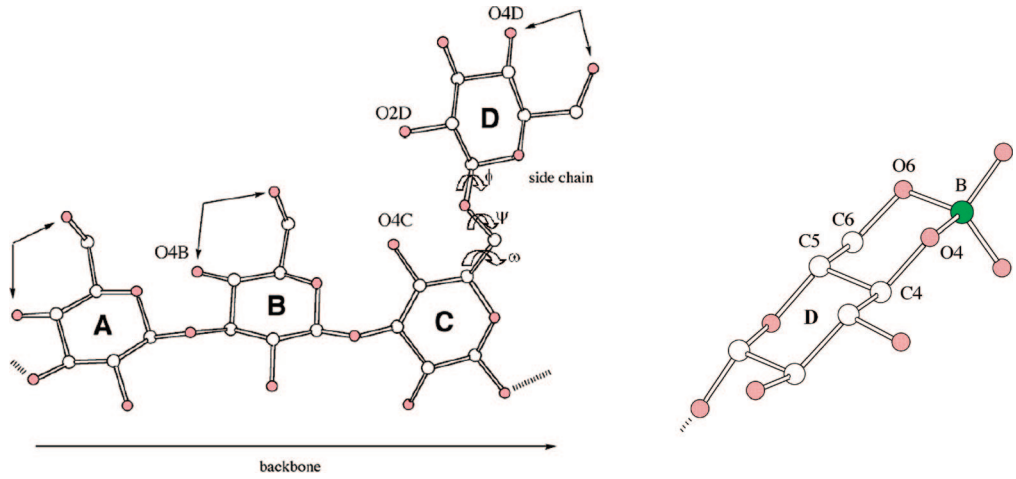

Figure 1. (left) Sclg repeating unit formed by three β-(1 → 3)-D-glucopyranose residues (A−C) and one branched β-(1→6)-D-glucopyranose (D). The oxygen atoms discussed in the text are labeled. The double arrows indicate the couple of atoms that can be involved in a borax 4–6 type linkage. (right) Example giving the structure of the side-chain glucose linked with borax at position 4–6. The boron, oxygen, and carbon atoms are shown as green, red, and white circles, respectively. The H atoms are omitted.

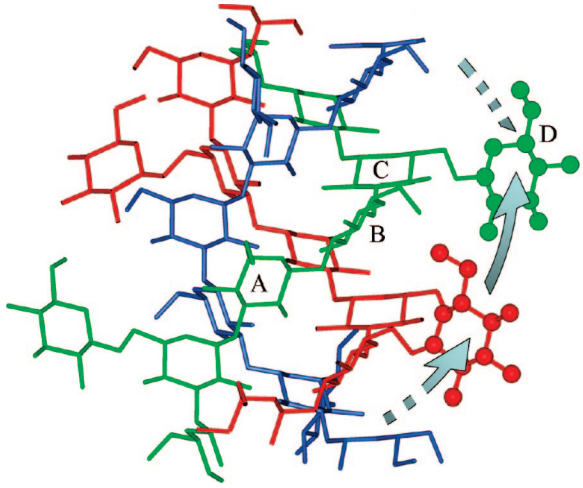

Figure 2. Fragment of the triple helix of Sclg. The view is perpendicular to the helical axis (side view). The three strands are colored red, blue, and green. As examples of residues involved in the structural transition at 280 K, two nearest neighbor glucose rings, belonging to two different strands, are shown as balls and sticks and connected by a cyan arrow.

to form nanochannel-like structures; the proposed model was able to explain the observed changes in the drug-release properties.

Nanochannel structures (or superstructures) formed by different materials (like carbon nanotubes,[17,18] protein in the solid state,[19–21] inorganic materials,[22] etc.) are well-documented and also their investigations by MD techniques have been reported.[23–28] It is well-known that the confinement, induced by a nanochannel, strongly affects the behavior of the solvent buried in the channel. In particular, the water diffusion coefficient (D) upon constraints can change its value and tends to become anisotropic. The presence of a channel can change the mechanism of diffusion, from classical Fickian behavior, observed in bulk water, to alternative mechanisms as single-file diffusion or ballistic motion. These mechanisms of diffusion are well described in the literature,[23,24,26,29–32] and it is possible to distinguish among them by monitoring the mean square displacement (MSD), dr^2, as a function of time. In fact, dr^2 is proportional to dt^{α}, where α is 0.5, 1, or 2 for single-file, Fickian, and ballistic motion, respectively.

Numerous investigations have reported the influence of different kinds of confinement on the static and dynamic properties of water molecules by means of computational techniques. The solvent behavior, in the presence of different geometrical restrictions (i.e. channels at different diameters[23,33–36] or slabs at different distances[31,37–39] and/or different chemical groups (i.e. hydrophobic or hydrophilic surfaces, presence of charged groups[25,40,41]), was analyzed; however, it is difficult to obtain general rules able to describe these phenomena. This, in a confined system, seems to be a consequence of the strong influence of the interfacial effects that can dramatically change with small variations of physicochemical properties. Furthermore, when the confinement reaches the dimension of a few water molecule layers (i.e., the situation with water molecules inside nanotubes with diameters below 1 nm), the ability of water to freeze in ordered structures can be strongly depleted also at very low temperatures (e.g., it has been experimentally shown that water does not freeze, even at 77 K, when confined in nanopores[42]).

The aim of the present paper is to characterize the locally ordered structures of Sclg chains induced by borax in which the stiff triplexes arrange in a parallel configuration promoting the formation of nanochannel-like structures. The channels thus formed are different with respect to those previously described, mainly because the confinement of water inside the channel is obtained by means of a "soft wall"; that is, the triplexes assembled by physical interactions. To support the MD simulations, DSC and AFM measurements were also carried out.

2. Materials and Methods

2.1. Materials. Sclg (Actigum CS11, Mero-Rousselot-Satia, France) was used after purification. A given amount of polymer was dissolved in distilled water and then kept under magnetic and mechanical stirring for 24 h. The obtained solution was exhaustively dialyzed at 280 K against distilled water with dialysis membranes having a cutoff of 12 000–14 000 and then freeze-dried. The lyophilized product was stored in a desiccator until use.

The appropriate amount of Sclg was dissolved in distilled water by continuous stirring for 24 h. A calculated amount of 0.1 M borax ($Na_2B_4O_7 \cdot 10H_2O$; Carlo Erba, Italy) was then added (i.e., moles of borax = moles of repeating unit of Sclg) to the polymer solutions. The mixture was magnetically stirred

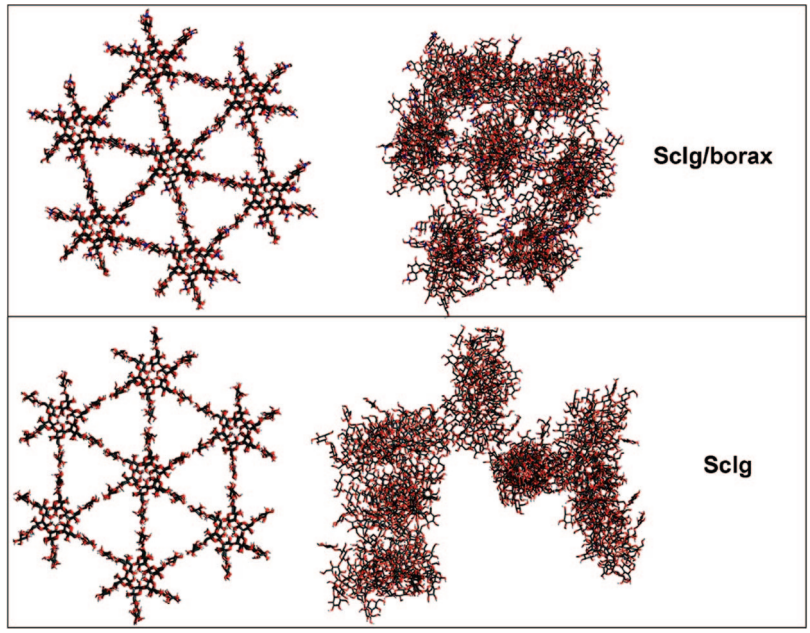

Figure 3. Top view of the starting (left) and final (right) structures in the simulation of seven triplexes with (top) and without (bottom) borax.

for 5 min and then left overnight for gel setting. The final polymer concentrations (c_p) were 0.07% (w/v) for the AFM samples and 0.70% (w/v) for DSC experiments.

2.2. Molecular Dynamic Simulations. MD simulations were performed with the GROMACS software package.[43–45] The force field parameters used were those obtained in previous works, both for saccharidic[5] and for borax moieties.[16]

The system with three triplexes has six Sclg repeating units for each strand (total of 225 glucose rings). About 13 000 water molecules (SPC model[46]) and 51 Na^+ ions (to balance the negative charges of borax groups) were added in a box of dimensions 7.7 × 8.2 × 7.0 nm.

In the Sclg/borax simulations, the borax groups were added to Sclg to form borinane groups (see Figure 1, right) as already reported (at the positions indicated by arrows in Figure 1, left).[16] The triplexes were disposed at a distance of about 3.0 nm from each other, in a parallel alignment. As can be easily recognized (see, for example, Figure 3 and left side of Figure 5), in such an arrangement the triplexes form a nanochannel-like structure whose axis is parallel to the triplex axes.

In the simulations with seven triplexes (i.e., 525 glucose units), more than 16 000 water molecules were added; for the simulation with borax, also 119 Na^+ ions were included in a box of dimensions 8.4 × 9.7 × 7.2 nm.

The simulations were performed according to a procedure previously described[47] with a few exceptions: (a) the electrostatic treatment was carried out by applying the PME method with a cutoff of 0.9 nm; (b) the LINCS algorithm was used to constrain the bond length; (c) the simulations were 5 ns long. The results of the first nanosecond of the overall MD simulation were discarded, in order to allow the relaxation of intertriplex strains. Also, the first and the last Sclg repeating units for each strand were not considered during analyses, due to their tendency to unwind in short tracts of Sclg triplexes.[6] For the same reasons the water molecules located 2 nm from the top and the bottom of the box along the *Z* direction were not included in the solvent analysis.

Root-mean-square positional fluctuations (RMSF), root-mean-square deviations (RMSD), mean-square displacements (MSD), radial distribution functions (RDF), angle correlations and square distance autocorrelation functions were calculated according to the standard definitions.

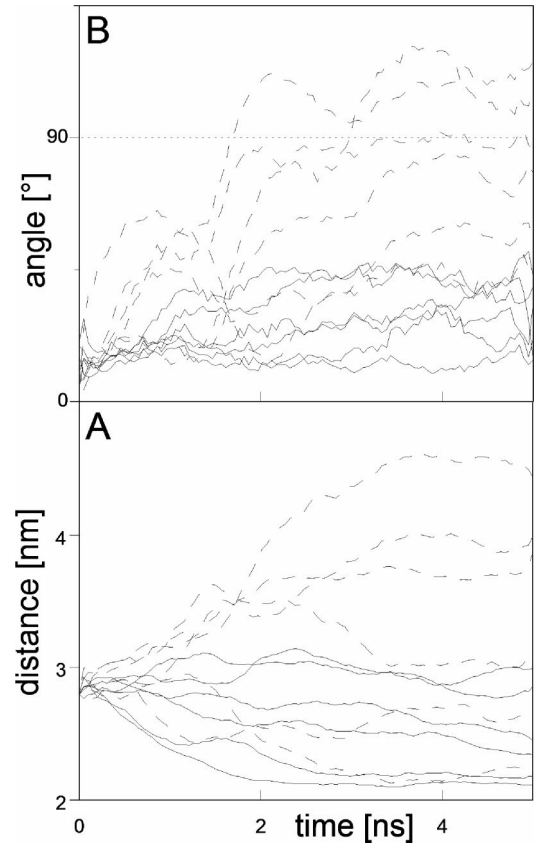

Figure 4. Angles between the helical axes (B) and distances of center of masses (A) for the central triplex and each peripheral triplex, over time, in the simulations of seven triplexes with (solid lines) and without borax (dashed lines).

The autocorrelation functions for the distance between oxygen atoms of water molecules (OW) were evaluated for contiguous 100 ps intervals from 1 to 5 ns for distances lower than 0.6 nm, corresponding approximately to the second peak in the OW-OW RDF.

The estimated square distances between two oxygen atoms of water molecules were obtained according to the equation

$$d^2_{estim}(t) = d^2_{start}(t_0) + 2[MSD(t)] \quad (1)$$

where $d^2_{estim}(t)$ represents the more probable square distance between two points, originally distant $d_{start}(t_0)$, after a movement of MSD(t).

Starting from the values of $d^2_{start}(t_0)$, at the beginning of the intervals, and $d^2_{estim}(t)$, calculated in steps of 1 ps up to 100 ps, the estimated square distance autocorrelation was obtained.

We used the MSD obtained from the simulation and averaged from 1 to 5 ns. In this interval the MSDs showed a linear trend, with values (at 100 ps) of 0.75 nm^2 for OW in the nanochannel and 2.56 nm^2 in the bulk.

The side-glcps and triplex orientations were obtained from the perpendiculars to the planes formed by C1D, C3D, and C5D atoms (for side-glps) and from the three O2 atoms involved in the interstrand H-bonds (for triplex).

The self-diffusion coefficient (D) was evaluated according to eq 2

$$D = \lim_{\Delta t \to \infty} \frac{\langle |\vec{r}_i(t) - \vec{r}_i(0)|^2 \rangle}{2\delta \cdot \Delta t} \quad (2)$$

where $\langle |r_i(t) - r_i(0)|^2 \rangle$ is the MSD and δ, ranging from 1 to 3, is the dimensionality of the considered system.

The anisotropy (A) of water diffusion inside the nanochannel, present in Sclg/borax simulation, was calculated according to

$$A = \frac{D_\perp}{D_\parallel} \quad (3)$$

where $D_\perp$ and $D_\parallel$ represent the self-diffusion coefficients calculated along the nanochannel direction and in the perpendicular plane, respectively.

In the solvent analysis, all the water molecules having an OW−O(Sclg) distance less than 0.35 nm are considered as surrounding.

2.3. AFM Experiments. A small volume, about 15 μL per drop, of the Sclg or Sclg/borax sample ($c_p = 0.07\%$) was drop-cast onto freshly cleaved mica sheets. The samples were then dried with a nitrogen flux for few minutes and immediately analyzed by using scanning force microscopy (SFM).

Tapping mode scanning force microscopy[48,49] was employed, recording both the height signal (output of the feedback signal) and the phase signal (phase lag of the oscillation relative to the driver). While the first type of image provides a topographical map of the surface, the latter is extremely sensitive to structural heterogeneities on the sample surface, therefore being ideal to identify different components in a hybrid film.[50] A commercial instrument (Multimode/Nanoscope IIIa, Digital Instruments, Santa Barbara, CA) was run in an air environment at room temperature with scan rates of 1–1.5 Hz/line. The analyses were operated in both dynamic and static modes. Under the dynamic conditions (tapping, lift mode, and attractive regime), commercially available etched silicon probes (Digital Instruments) with a pyramidal shape tip having a nominal curvature of 10 nm and a nominal internal angle of 35° were used. During scanning, the cantilever, 125 mm long, with a nominal spring constant in the range of 20–100 N/m, oscillated with its resonance frequency (330 kHz). Images with scan lengths ranging from 5 μm down to 0.5 μm have been recorded with a resolution of 512 × 512 pixels, and the scan rate was maintained below 1 line/s. In the static modes (contact and friction), silicon nitride tips (Digital Instruments) with a nominal tip radius of 20–50 nm were used. These experiments were performed with a cantilever having a nominal spring constant of 0.12 N/m. The scan rate ranged from 2 to 4 lines/s.

The analysis off-line of the images has been carried out using the software "Scanning Probe Image Processor (SPIP)" (version 5.12r3 supplied by the manufacturer). The half-widths have been calculated on 150 points for each sample.

2.4. DSC Experiments. The hydrogel obtained with Sclg/borax ($c_p = 0.7\%$) was placed in the differential scanning calorimetry (DSC) cell. As a comparison, a solution of Sclg ($c_p = 0.7\%$) without borax was also investigated. DSC measurements were carried out with a microcalorimeter (Micro-DSC III, Setaram, France) using a scan rate of 0.2 K/min. Samples of approximately 803 mg were hermetically sealed in the vessel with water used as a reference. The samples were heated and cooled between 0.2 and 14 °C. The excess heat capacity, $C_{p,exc}$, i.e. the apparent heat capacity exceeding the baseline drop across the transition (sigmoid line connecting onset and offset of the signal), was obtained as already reported in the literature.[51] The runs were performed according to a heating–cooling cycle. The overall melting enthalpy was obtained by integrating the excess heat capacity within the explored temperature range, as already described in the literature.[52]

3. Results and Discussion

3.1. Stability of Sclg/borax Nanochannels. As a first attempt, we simulated a system with three triplexes containing most glucose residues linked with borax. Even if couples of triplexes tend to remain stable during simulation, confirming the results obtained in a previous work,[16] the starting conformation, with the three triplexes arranged in a channel like form, is definitively lost. These results are summarized in Figure S1 in the Supporting Information.

Probably a scale factor plays an important role in the aggregation processes of the three triplexes, at least under the simulation conditions (short triplex tracts), that are not able to ensure stability to the nanochannel system. For these reasons, as a second attempt to obtain a stable nanochannel, we tested a system with seven Sclg/borax triplexes (and six nanochannels). The starting geometry reflects the intrinsic symmetry of triplexes, in which the side-glcps are present every 60° (see Figure 3).

In this case, RMSD values of the single triplexes do not show valuable differences between Sclg and Sclg/borax simulations (see Figure S2 in the Supporting Information), confirming the intrinsic stability of the triple-helical structure as reported in previous papers.[5,16] In contrast, the behavior is markedly different when the intertriplex interactions are investigated. The channel-like starting configuration is retained in the simulation with borax, whereas the system without borax evolves toward a disordered state where the original order is completely lost.

Figure 4A reports the distances between the centers of mass of the central triplex and each of the peripheral triplexes during both simulations. In the Sclg/borax simulation in two cases the distances oscillate around the imposed value, whereas the other four stabilize at lower values between 2.1 and 2.5 nm. On the other side, without borax, in four cases the triplexes appear totally independent from the central triplex and the distances increase up to 4.6 nm with large oscillations. To ensure a channel-like structure, it is important to have the correct orientation among the triplexes. Figure 4B reports the angles between central and peripheral triplexes in both simulations. In spite of the shortness of the simulated tracts (that could promote anomalous tilt not present in real samples), in the simulation

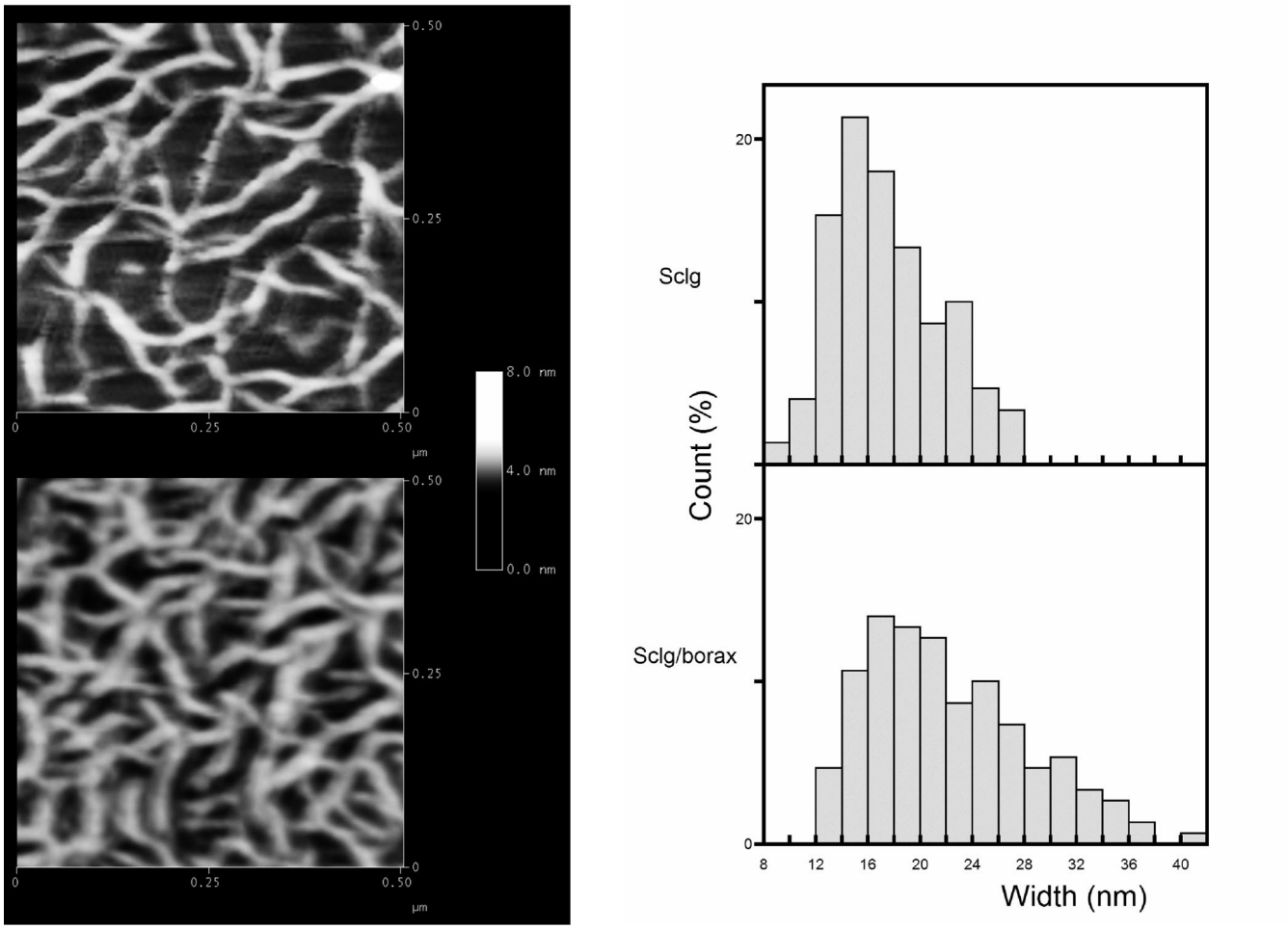

Figure 5. (left) AFM images of Sclg (top) and Sclg/borax (bottom). (right) Width distributions obtained from AFM analysis.

with borax the system is able to retain the original orientation with values that never exceed 45° with small oscillations during simulation time. The Sclg simulation exhibits a different behavior with angles that in four cases are near 90° (i.e., the triplexes assume a perpendicular orientation with respect to the central one), and in all cases the angles show high variability.

3.2. AFM Study of Scleroglucan Structure Organization. In order to experimentally confirm these results, we acquired nanoscopic images of our system by means of scanning force microscopy (SFM). The objective of these investigations was to study the structural organization of Sclg in the presence of borax and not to acquire information about single Sclg/borax triplexes. For this reason we carried out these experiments starting from concentrations higher than those usually used.[53] Because the presence of a high number of entanglements in the gel could strongly impair the interpretation of AFM images, the concentrations used were lower than those usually used for gel formation. An example of the collected images for Sclg and Sclg/borax are shown in Figure 5. Sclg shows a width equal to 18 ± 4 nm and a height of 1.2 ± 0.3, similar to those obtained by different authors for a single Sclg triplex.[53] A significant increase in the population at higher width (see right side of Figure 5) is observed in the case of Sclg/borax. This is a clear evidence that the borax acts to promote the aggregation of triplexes, even at low concentrations.

3.3. Effect of Confinement on the Sclg Flexible Region. As already reported, the Sclg structure consists of a triple-helix backbone (core), strongly stabilized by a network of interchain H-bonds, and of external side-glcps linked β-(1→6). Such a peculiar conformation shows high stability, stiffness, and low mobility of atoms belonging to the core region. On the other hand, the high flexibility, typical of residues linked 1 → 6, is only slightly depleted from the presence of the triplex superstructures.[5]

As shown in Figure 6, reporting the RMSF of carbon atoms belonging to the central triplexes of simulated systems with seven triplexes (with and without borax), the presence of borax, and, consequently, of nanochannels, strongly reduces the atom mobility. In both simulations the carbon atoms show different degrees of mobility if they belong to the core (RMSF values below 0.1 nm) or to the side-chain regions (the 12 peaks appear every 24 atoms). However, a lower RMSF value is evident for all the carbon atoms of Sclg/borax, and in particular the difference appears larger for those of the side chains. Such results strongly suggest that a lower mobility is induced by confinement, in particular for the side-glcps. This can be a consequence of the nanochannel-like structure that is substantially retained with borax, while it is lost without borax.

In order to analyze the mobilty of side-glcps of the central triplex, we monitored during our simulations either the ω torsional angle, the more flexible of the three angles of the bridge side-core (see Figure 1), or the angle between the average plane of each side-glcp and the triplex axis.

In particular, when the transitions of the ω angles of side-glcp belonging to the core region of the central triplex (12 angles) in the time range between 1 and 5 ns were analyzed, 7

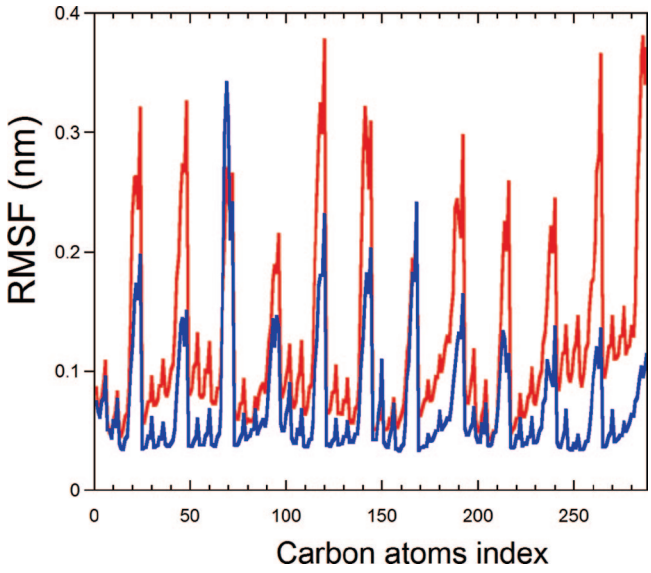

Figure 6. Root-mean-square fluctuations (RMSF) of carbon atoms in the central triplexes, as obtained from simulations of Sclg/borax (blue curve) and Sclg (red curve). The terminal regions of the triplexes have not been taken into account, and the first nanosecond of simulation is excluded.

transitions between different minima for Sclg/borax (0.14 transition/ns) and 15 transitions for Sclg (0.33 transition/ns) were detected. The latter frequency is close to those previously reported for a single triplex,[5] whereas the former frequency is definitely lower.

As representative of side-glcp mobility, we have monitored also the standard deviations of the angles between each side-glcp belonging to the core region of the central triplex and its axis. Variations of this parameter are mainly related by ω angle transitions, but they can be also a consequence of ϕ and ψ angle mobility (see Figure 1). These data, in both the presence and absence of borax, are reported in Table 1. Sclg shows both higher angular fluctuations and higher heterogeneity (values ranging from 13.5 to 48.8). This last effect can be due to some glucose units that remain in tight contact with other triplexes, while other glucose units are completely exposed to the solvent (see the final structure in Figure 3). On the other side, in the presence of borax, all the side-glcps of the central triplex remain in the same environment.

Furthermore, from the data of Table 1 it can be observed that in the Sclg/borax simulation there is not much difference among the mobilities of side-chain glucose units esterified with borax (4, 7, and 12), and those of the other units belonging to the same triplex but not linked to borax. This evidence allows us to assert that the lower mobility in the Sclg/borax system is mainly due to the confinement induced by the formed nanochannels and cannot be considered as a direct consequence of the presence of borax.

As already reported, several authors proposed that the conformational transition, experimentally detected at 280 K, is connected with the conformational freedom degrees of side-glcps and, in particular, that their motions should be mediated by the first shells of hydration.

Since our simulations were carried out at a temperature higher than that of the transition, we do not aspect to find a fully extended correlation of these motions. However, a comparative analysis of correlation between nearest couples of side-glcps in the two simulated systems (with and without borax) can give useful information regarding the tendency to undergo the aforementioned transitions. These couples of glucoses, belonging to different strands, describe a superhelical motif around the triplex (see Figure 2), and they are no more than 1.5 nm apart from each other.

As can be seen from Table 2, with borax the movement of the side chains is completely uncorrelated, with values that never exceed 0.23. An opposite effect is detected in Sclg, where the local correlations sometime reach a high value (up to 0.7 in two cases). As emphasized above, such a correlation is never fully extended but is restricted only to couples of the nearest glucose units because, as discussed earlier, the simulations are carried out at a temperature higher (300 K) than that of the transition (280 K), where these motions are frozen. Furthermore, it is known that the fully extended correlation of this motion is hard to simulate, probably due to the shortness of the Sclg triplexes considered, also at a lower temperature (273 K).[5,6] Nevertheless, the higher local correlation in Sclg with respect to Sclg/borax, at 300 K, could reflect the major tendency of Sclg to undergo this transition.

To summarize, the presence of borax induces two effects on the side chains of the Sclg triplex: (a) a strong reduction of their mobility and (b) a decrease in the mobility correlations for the nearest neighbor glcp residues that could represent a noticeable hindrance to the highly cooperative transition.

To experimentally verify the consequences of the presence of borax on such a transition, we carried out DSC experiments on Sclg and Sclg/borax samples (see Figure 7). As can be observed from the thermogram, Sclg/borax does not show the characteristic peak of Sclg, thus supporting the hypothesis that the correlation among the side chains represents the most important factor related to the conformational transition.

3.4. Influence of Soft Nanochannels on the Solution Properties. Until now we have discussed the main effects of borax on the flexible region of the Sclg triplex, especially those related to the conformational transition that takes place in the Sclg solution below 280 K. However, it is interesting to point out that, due to the presence of nanochannel-like superstructures, the Sclg/borax system is capable to influence the solvent properties. Numerous authors have already studied in detail the effects induced by systems with well-defined and rigid nanochannels. In our opinion, it is interesting to investigate the solvent behavior in our system, where the walls of the channels impair the free diffusion of solvent but are not completely impermeable.

To analyze the confinement effects on the solvent molecules, we need to distinguish among different kinds of water molecules present in our simulation box. The adopted criterion is described below. We consider a water molecule confined in the nanochannel if its oxygen atom lies at a distance lower than 1 nm from the central triplex (blue atoms in Figure 8A). A molecule at a distance higher than 1 nm from all the seven triplexes is considered as bulk water (red in Figure 8A). All the water molecules not considered in these two groups (green in Figure 8A), located at a distance less than 1 nm from the six peripheral triplexes, are actually influenced by the presence of triplexes but not by confinement effects. As already emphasized, all the water molecules in proximity of the flexible triplex terminals were not analyzed (Figure 8B). The distance of 1 nm has been chosen for comparison with the nanochannel dimension; a slight variation of this parameter does not change the main features of the analyzed properties. During the simulation the three groups of water molecules were updated every 10 ps. In this time scale only a small percentage of water molecules moves among the three groups considered: more in detail, less than 5% moves from the channel (blue in Figure 8) to the region

TABLE 1: Standard Deviation of the Angles between the Perpendicular to the Plane of a Side Chain Glucose Ring (Labeled as D in Figure 1) and the Triplex Axis Calculated for the Central Triplex

	strand I				strand II				strand III				
glucose[a]	1	2	3	4	5	6	7	8	9	10	11	12	av
Sclg/borax	11.9	15.2	19.5	13.0[b]	11.8	19.3	15.5[b]	19.4	14.7	17.1	16.1	13.7[b]	15.6 ± 2.8
Sclg	33.3	34.5	39.6	15.0	17.1	32.8	30.5	48.8	13.5	19.8	30.9	23.6	28 ± 11

[a] The glucose rings belonging to the terminal residues are omitted. [b] Rings esterified with borax.

TABLE 2: Correlation between Plane Movements of a Pair of Nearest Neighbor Side-glcps in the Central Triplex, Excluding the Terminal Regions[a]

simulation	av value[a]	max value	no. of values in the range 0.2–0.3	no. of values >0.3
Sclg/borax	0.07 ± 0.05	0.23	1	0
Sclg	0.23 ± 0.14	0.69	3	7

[a] The side-glcp plane movement is obtained by monitoring the angle between its perpendicular and the helical axis.

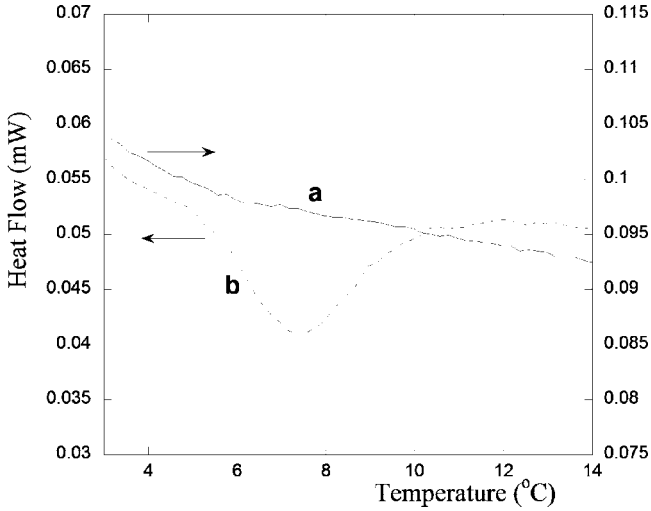

Figure 7. Differential scanning calorimetry (DSC) curves for Sclg/borax (solid line) and for Sclg (dashed line).

surrounding the peripheral triplexes (green in Figure 8) and no molecules move from channel to bulk (red in Figure 8).

First of all, we analyzed the influence of confinement on the diffusion coefficient (D). Figure 9 shows D values, as a function of time, for the three types of water molecules considered above. The average value calculated for bulk water molecules is $(4.6 \pm 0.2) \times 10^{-5}$ cm^2/s, close to the experimental value of 5.2×10^{-5} cm^2/s.[54] The small difference between the two values depends on the adopted model (SPC), which is known to give a lower value when compared to the experimental system (a smaller value, equal to 4.3×10^{-5} cm^2/s, is reported under slightly different conditions[55]).

Thus, the water molecules at a distance of more than 1 nm are not influenced by the presence of the triplexes, while an average diffusion constant of $(3.0 \pm 0.1) \times 10^{-5}$ cm^2/s is estimated for the water molecules closer than 1 nm to the peripheral triplexes. This reduction is not surprising, as it is already known that saccharidic molecules can influence the surrounding solution.[56,57] The influence of saccharidic moieties is amplified for water molecules inside the nanochannels formed by different triplexes (blue). In this case the average D value is $(1.5 \pm 0.2) \times 10^{-5}$ cm^2/s, with a reduction of about 70% with respect to the bulk value. This effect is clearly due to the simultaneous presence of more triplexes that produce a confinement effect on the water molecules present inside the channel. This kind of behavior was already reported in MD simulations of water in carbon nanotubes. In particular, a diffusion decrease was observed for water molecules inside hydrophilic nanotubes, while the opposite behavior was detected for water molecules inside hydrophobic nanotubes.[35,41]

We also analyzed the diffusion of water molecules, assigning their type after the first nanosecond, without reassigning them during simulation (dashed curves in Figure 9). In this case, the water molecules indexed as belonging to a group can move during simulation toward other regions in the box. As shown in Figure 9, the diffusion coefficients for the three groups converge toward the same value (about 3.7×10^{-5} cm^2/s), indicating that during the simulated interval of time (4 ns) the molecules are completely shuffled. Water molecules can leave a nanochannel through the base or through its lateral wall. The first mechanism has to be considered as an artifact of simulation, as the actual triplexes (and consequently the real nanochannel) are longer than the simulated system, while the second mechanism is the one that actually could occur within the studied system. When the changes of water molecule coordinates are tested, both mechanisms are detected and about 63% of water molecules left the nanochannel passing through the boundaries. Thus, also if the calculated relaxation time (on the order of nanoseconds) should be considered a lower limit, most likely the diffusion of water molecules through the channel walls takes place, in this system, on the same time scale (nanoseconds). For this reason the Sclg/borax system can be considered as a *soft* nanochannel.

It is well-known that the confinement effect can perturb the solvent diffusion behavior, introducing non-Fickian or anisotropic diffusion.[19,23,24,31,35,54,58] Below we shall discuss both of these aspects.

In Figure 10 the MSDs calculated within an interval of 10 ps, and averaged during the trajectory, are reported. As can be seen, there is a linear relationship between the MSD and time, indicating that the Fickian behavior is not perturbed for the three kinds of water, even for water molecules in the nanochannels. As a comparison, in Figure 10 the data obtained from the simulation without borax, where the channels are absent, are also reported. The bulk water behavior (namely, water molecules at a distance higher than 1 nm from each triplex) is practically indistinguishable in the two cases. When the water molecules surrounding the central triplexes are considered, a remarkable MSD difference is detected between the Sclg and Sclg/borax simulations. The water molecules surrounding the central triplex in the Sclg simulation (where the channel is absent) are similar to those surrounding the peripheral triplexes in the Sclg/borax simulation (near the triplex but not in a nanochannel). Consequently, it is not surprising that, in both cases, the same D reduction (about 30%, obtained from the slopes of the curves) is detected with respect to the bulk water, suggesting that the borax has, per se, no influence on the MSD. A major effect, as already reported, is observed in the simulation with borax for water molecules inside the *soft* channel, which showed a further decrease of MSD slope.

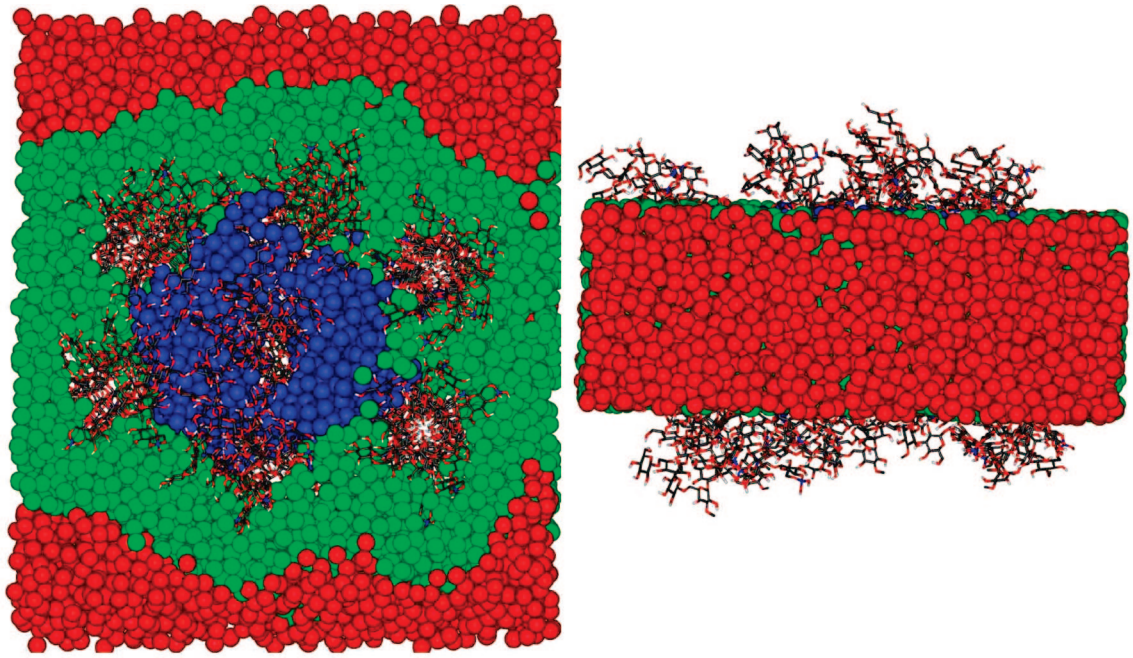

Figure 8. Top (left) and side (right) views of an Sclg/borax simulation box at 3 ns. The polysaccharide bonds are represented as sticks. The oxygen atoms of the water molecules (OW) with *Z* coordinates between 2 and 5 nm are shown as spheres. The OWs at a distance lower than 1 nm from the central triplex are shown in blue (water molecules in the nanochannels). The remaining ones are shown in green if they lie at a distance less than 1 nm from the six peripheral triplexes (water molecules near the peripheral triplexes) or red if they are at a distance higher than 1 nm from the atoms of each triplex (bulk water molecules). The remaining OWs, present in the simulation but not analyzed, are not reported.

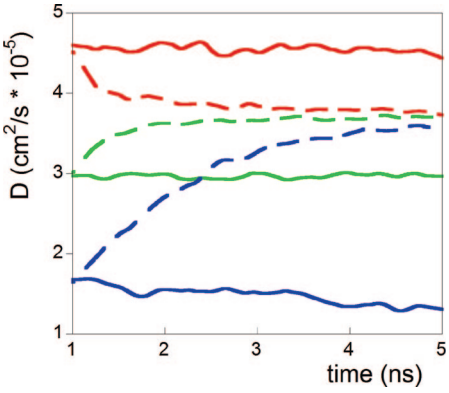

Figure 9. Coefficient of diffusion (*D*) vs time for Sclg/borax. The reported data are calculated with a Δt value of 10 ps and refer to the three kinds of water molecules described in Figure 8. As in Figure 8, the blue lines refer to water molecules inside the nanochannels, the green lines to molecules near the six peripheral triplexes, and the red lines to bulk water molecules. The solid lines are calculated by reassigning the water molecules at the three groups every 10 ps during the simulation. The dashed lines are calculated by assigning the water molecules at the three groups only at 1 ns.

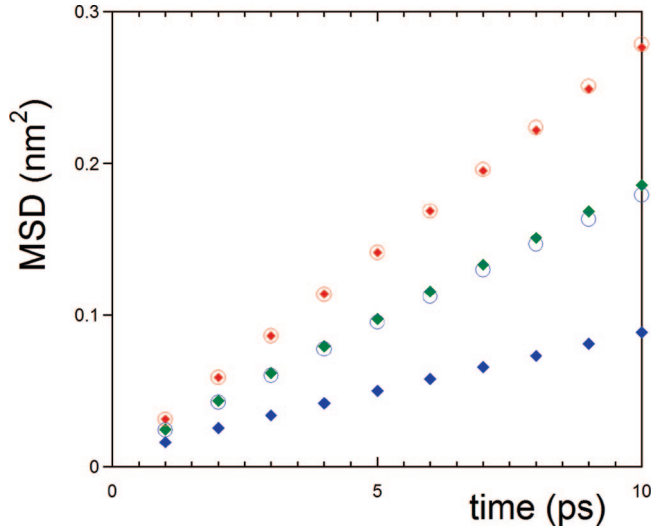

Figure 10. Mean square displacements (MSD) for OW atoms. The average values, calculated at contiguous 10 ps intervals from 1 to 5 ns of simulation, are reported. The three sets of data reported as filled rhombuses are calculated for the Sclg/borax system and refer to the three groups of water molecules described in Figure 8, adopting the same color code. The data reported as hollow circles are calculated for the Sclg system; in this case, the blue symbols refer to molecules at a distance less than 1 nm from the triplex that is central in the starting configuration and the red circles refer to bulk water molecules (distance more than 1 nm from each triplex).

Figure 11 reports the diffusion anisotropy measured in the last nanosecond simulation with borax. The bulk water molecules, as expected, show an isotropic behavior, while the water molecules buried in the nanochannel exhibit a significant anisotropy in the diffusion.

This result is typical of water molecules confined into "hard walls", and it clearly supports the nanochannel-like structure proposed for our system, even if a strictly rigid confinement is not present. More quantitatively, anisotropies of about 15–20%, as found for the Sclg/borax system, have been already predicted in nanochannels of protein crystals with a ratio between solvent and channel diameters of about 0.3.[19]

Furthermore, it was demonstrated that the confinement effect influences the formation of solvent aggregates.[26,28,30,59] This aspect is particularly important for the Sclg/borax system, where the conformational transition, detected at 280 K for Sclg, is absent (see Figure 7), considering that clusters of water molecules mediate this transition. As a consequence, each factor promoting different kinds of water ordering could impair the considered transition.

The existence of clusters of water molecules was tested by evaluating the square distance autocorrelation function of the

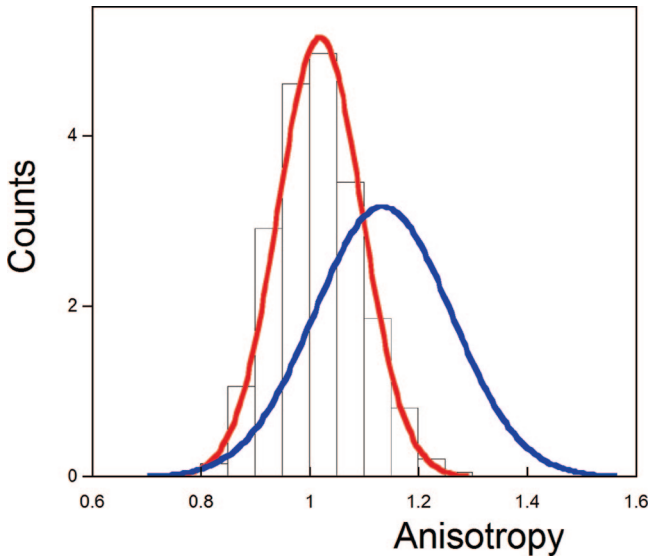

Figure 11. Fitting curves of anisotropy distribution, calculated at contiguous 10 ps intervals in the last nanosecond of Sclg/borax simulation. The two curves refer to water molecules in the nanochannel (blue curve) and in the bulk (red curve) (see also Figure 8). For the sake of clarity the original data are reported only for bulk water molecules (black lines).

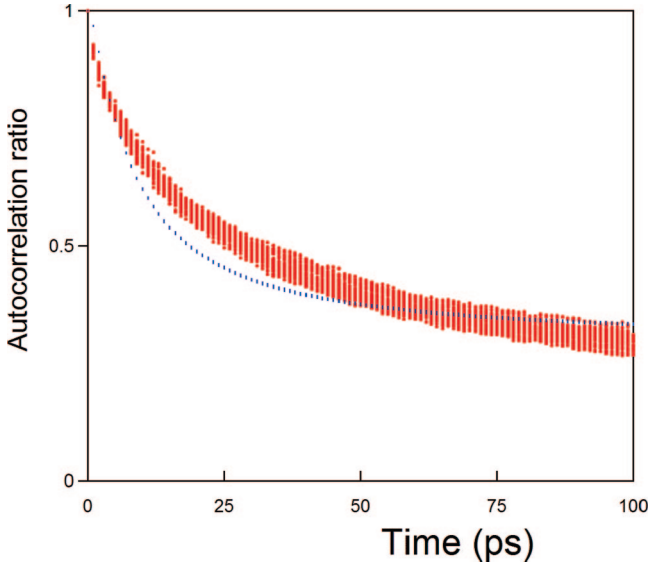

Figure 12. Ratio between the square distance autocorrelation functions for OW atoms in the bulk and in the confined region for the Sclg/borax (excluding those at a distance less than 0.4 nm from Sclg). The red points were obtained from the simulation considering contiguous 100 ps intervals from 1 to 5 ns. Blue points are the corresponding estimated values.

oxygen atoms of water molecules located inside the nanochannel or in the bulk solution in a time range of 100 ps.

The ratios between the autocorrelation functions calculated in the bulk and in the confined region, together with the corresponding estimated value, are reported in Figure 12. The estimated values were obtained, as described in Materials and Methods, by correlating the starting distances (in the considered intervals of 100 ps) with the expected distances (predicted on the basis of MSD values) at different times (see eq 1). As shown in Figure 12, the predicted ratio nicely agrees with that obtained from the simulation. This result suggests that the nanochannel does not promote, significantly, the formation of water clusters at 300 K. Consequently, the absence of the conformational transition appears to be unrelated to the presence of an alternative order of water molecules promoted by confinement in the Sclg/borax system. Other aspects should be taken into account to better explain these results.

TABLE 3: Diffusion Coefficients (D) of Water Molecules Surrounding Different Atoms of the Central Triplex

molecules	D (10^{-5} cm^2/s)[a]	
	Sclg/borax	Sclg
1 nm from the central triplex[b]	1.3 ± 0.1	2.9 ± 0.2
near O4C atoms[c]	0.5 ± 0.2	1.0 ± 0.4
near O2D atoms[c]	0.8 ± 0.3	1.6 ± 0.5
near O4B (free) atoms[d]	0.6 ± 0.3	
near O4B (linked with borax) atoms[e]	0.1 ± 0.1	

[a] Data were calculated at contiguous 100 ps intervals from 1 to 5 ns. [b] These data are reported as references. For Sclg/borax simulation they refer to water molecules in the nanochannels and for Sclg to water molecules near a triplex. [c] 12 oxygen atoms in the considered region. [d] 7 oxygen atoms in the considered region. [e] 5 oxygen atoms in the considered region.

In a previous paper[5] we showed that the water molecules nearest to the Sclg oxygen atoms behave differently when the temperature in the simulation was decreased. In particular, the water molecules surrounding the oxygen atoms belonging to the core (first shell of triplex hydration) are less influenced than those interacting with oxygen atoms of side-glcps (second shell of triplex hydration). The behavior of these water molecules in the system with and without borax, considering that the slower diffusion of water molecules buried in the nanochannel can be roughly assimilated to a decrease of temperature, is now analyzed. In this study only the diffusions of the molecules at a distance up to 0.35 nm from O4C and from O2D atoms in the last nanosecond of simulation were considered. These atoms have been chosen as representative of the oxygen atoms in the core and in the side chain, respectively, because they are never involved in the chemical linkages with borax.

The results, reported in Table 3, can be summarized as follows: (a) as expected, for both systems, Sclg and Sclg/borax, a significant reduction of the diffusion coefficient is observed for water molecules closer to the triplex in comparison to those of the bulk; (b) in the presence and in the absence of borax the water molecules belonging to the first shell of hydration (near the O4C atoms) diffuse less than the more external ones (near the O2D atoms); (c) a decrease of diffusion is induced by borax, but it does not produce any specific effect on the molecules of the second shell (as already found in the simulation of Sclg at a lower temperature).[5]

Furthermore, to test the influence of borax on the surrounding solvent, the diffusion of water molecules nearest to oxygen atoms esterified or not esterified with borax was monitored. In particular, we calculated the diffusion coefficient D for water molecules belonging to the first shell of hydration near the O4B atoms. As shown in Table 3, the water molecules surrounding the oxygen atoms linked with borax show a relevant decrease in the diffusion coefficient.

For a deeper insight into this effect, the radial distribution function (RDF) of water molecules surrounding the O4B atoms was analyzed. The two types of such atoms, i.e. linked or not linked to borax, were tested in the simulation, and the obtained results are reported in Figure 13.

The two curves refer to atoms located in the same region of the box simulation; thus, the differences are due to the presence of borax, which strongly orders the surrounding water molecules.

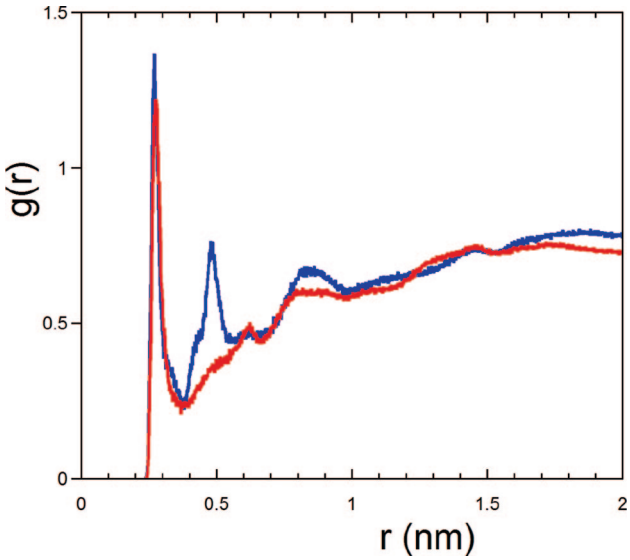

Figure 13. Radial distribution function (RDF) between OW and O4B (free) atoms (red line; seven atoms excluding the triplex terminal regions) and between OW and O4B (linked with borax) atoms (blue line; five atoms, excluding the triplex terminal regions). All data refer to atoms in the central triplex of Sclg/borax simulation.

Two peaks, corresponding to the second and third hydration shells, are well-defined for the O4B atoms linked with borax. These results can be related to the correlation decrease observed for the side-chain glucose ring movements described above (see Table 2) and, as a consequence, to the absence of the conformational transition at 280 K. The presence of borax in a random position along the triplex promotes the formation of well-ordered water molecule domains. This effect should destabilize the water molecule structure present in Sclg that, in some way, is responsible for the side-glcps correlation.

Finally, the behavior of 119 Na^+ counterions present in the simulation with borax was analyzed. When their mobility during the last nanosecond is considered (data not reported), it appears that a group of ions is practically "frozen" near the borax (negatively charged), while other ions show mobility somewhat comparable to that of water (D up to 3.0×10^{-5} cm^2/s). Interestingly, the ions with the lowest mobility (9 out of 119 with RMSF < 0.15 nm) are located inside the channel (see Figure S3 in the Supporting Information). This suggests that the positively charged counterions are essential in stabilizing the interactions among the negatively charged triplexes. It should be emphasized that this effect is clearly given by the amount of Na^+ ions already present in the added borate, thus leading to the formation of the hydrogel even in water,[12] without the need to use additional salts to increase the ionic strength.[60]

4. Conclusion

In a previous work we demonstrated that borax stabilizes a parallel arrangement of two Sclg triplexes.[16] These results are now confirmed by means of AFM images showing that triplexes of Sclg can assume a parallel disposition in the presence of borax when deposited on the mica surface, even at concentrations lower than those required for gel formation.

The arrangement assumed by more than two triplexes has been analyzed by means of MD simulations. In the Sclg/borax system with seven triplexes, such triplexes remain near each other, thus stabilizing a nanochannel-like structure.

The simultaneous presence of several triplexes in a narrow space strongly influences the behavior of the flexible side chains of Sclg. In particular, the side-glcps, involved in the conformational transition detected at 280 K (in the absence of borax), showed a lower mobility compared with that observed in the simulation without borax. On the other hand, the correlation of motions for couples of nearest neighbor side-glcps is strongly impaired at 300 K in the presence of borax. Such correlation plays a key role in the aforementioned transition at 280 K, as confirmed in the DSC analysis showing that such a transition disappears in the presence of borax. It has been shown that this is a direct consequence of the presence of borax randomly located along the triplexes, which promotes a local order on the solvent molecules. This locally induced solvent structure near each borax probably perturbs the solvent order that in the Sclg mediates the correlation among the neighboring side-glcps extended along the triplexes, thus impairing the conformational transition. Furthermore, no evidence of water cluster formations inside the nanochannel, induced by confinement, has been detected.

If the absence of the conformational transition can be explained as a mere consequence of the presence of borax along the triplexes, other effects on the solvent properties appear to be a consequence of the superstructural organization of the Sclg triplexes induced by borax. In particular, the described nanochannel-like structures confine some solvent molecules in a narrow space. These solvent molecules can be assimilated to those constrained in a rigid nanochannel with hydrophilic walls (i.e., modified carbon nanotubes). The water molecules showed, indeed, a marked lowering of diffusion coefficient (about 70%) in comparison to bulk water and also an anisotropic diffusion along the channel axis. The nature of these nanochannels, obtained by means of physical interactions, is obviously rather different from that previously reported in the literature. As a consequence, these peculiar *soft* nanochannel walls strongly impair the free solvent diffusion, but they are not totally impermeable to water molecules.

Finally, the effect of Na^+ ions, added in the Sclg/borax simulations in a stoichiometric ratio to balance the negative charges introduced with borax, has been analyzed. The diffusion coefficients of the 119 Na^+ ions present in the system during the last nanosecond of simulation showed a wide heterogeneity, spanning from ions practically frozen near the borax atoms to ions with mobilities comparable with those of free solvent molecules. Interestingly, all frozen ions are located inside the nanochannel, suggesting their crucial role in the stabilization of the interaction among the triplexes, where the negatively charged groups of borax are present.

Acknowledgment. This work was supported by the MIUR PRIN/FIRB of Italy.

Supporting Information Available: Figures S1−S3, giving additional details of the study. This material is available free of charge via the Internet at http://pubs.acs.org.

References and Notes

(1) Giavasis, I.; Harvey, L. M.; McNeil, B. In *Biopolymers: Polysaccharides II*, De Baet, S., Vandamme, E. J., Steinbuchel, A., Eds.; Wiley-VCH: Weinheim, Germany, 2002; Vol. 6, pp 37–60.

(2) Norisuye, T.; Yanaki, T.; Fujita, H. *J. Polym. Sci., Polym. Phys.* **1980**, *18*, 547.

(3) Bluhm, L. T.; Deslandes, Y.; Marchessault, R. H.; Perez, S.; Rinaudo, M. *Carbohydr. Res.* **1982**, *100*, 117.

(4) Duus, J. O.; Gotfredsen, C. H.; Bock, K. *Chem. Rev.* **2000**, *100*, 4589.

(5) Palleschi, A.; Bocchinfuso, G.; Coviello, T.; Alhaique, F. *Carbohydr. Res.* **2005**, *340*, 2154.

(6) Kony, D.; Damm, W.; Stoll, S.; van Gunsteren, W. F.; Hünenberger, P. H. *Biophys. J.* **2007**, *93*, 442.
(7) Itou, T.; Teramoto, A.; Matsuo, T.; Suga, H. *Carbohydr. Res.* **1987**, *160*, 243.
(8) Yoshiba, K.; Ishino, T.; Teramoto, A.; Nakamura, N.; Miyazabi, Y.; Sorai, M.; Wang, Q.; Hayashi, Y.; Shinyashiki, N. *Biopolymers* **2002**, *63*, 370.
(9) Saito, H.; Yoshioka, Y.; Yokoi, M.; Yamada, J. *Biopolymers* **1990**, *29*, 1689.
(10) Teramoto, A.; Gu, H.; Miyazaki, Y.; Sorai, M.; Massimo, S. *Biopolymers* **1995**, *36*, 803.
(11) Yoshiba, K.; Teramoto, A.; Nakamura, N.; Shikata, T.; Milyazaki, Y.; Sorai, M.; Hayashi, Y.; Miura, N. *Biomacromolecules* **2004**, *5*, 2137.
(12) Coviello, T.; Grassi, M.; Lapasin, R.; Marino, A.; Alhaique, F. *Biomaterials* **2003**, *24*, 2789.
(13) Coviello, T.; Coluzzi, G.; Palleschi, A.; Grassi, M.; Santucci, E.; Alhaique, F. *Int. J. Biol. Macromol.* **2003**, *32*, 83.
(14) Coviello, T.; Grassi, M.; Palleschi, A.; Bocchinfuso, G.; Coluzzi, G.; Banishoeib, F.; Alhaique, F. *Int. J. Pharm.* **2005**, *289*, 97.
(15) Coviello, T.; Palleschi, A.; Grassi, M.; Matricardi, P.; Bocchinfuso, G.; Alhaique, F. *Molecules* **2005**, *10*, 6.
(16) Palleschi, A.; Coviello, T.; Bocchinfuso, G.; Alhaique, F. *Int. J. Pharm.* **2006**, *13*, 322.
(17) Iijima, S. *Nature* **1991**, *354*, 56.
(18) Hummer, G.; Rasaiah, J. C.; Noworyta, J. P. *Nature* **2001**, *188*, 414.
(19) Malek, K.; Odijk, T.; Coppens, M. O. *ChemPhysChem* **2004**, *5*, 1596.
(20) Margolin, A. L.; Navia, M. A. *Angew. Chem., Int. Ed.* **2001**, *40*, 2204.
(21) Vilenchik, L. Z.; Griffith, J. P.; St.Clair, N.; Navia, M. A.; Margolin, A. M. *J. Am. Chem. Soc.* **1998**, *120*, 4290.
(22) Giaya, A.; Thompson, R. W.; Denkewicz, R. J. *Microporous Mesoporous Mater.* **2000**, *40*, 205.
(23) Striolo, A. *Nano Lett.* **2006**, *6*, 633.
(24) Sholl, D. S.; Lee, C. K. *J. Chem. Phys.* **2000**, *112*, 817.
(25) Huang, L. L.; Zhang, L. Z.; Shao, Q.; Wang, J.; Lu, L. H.; Lu, X. H.; Jiang, S. Y.; Shen, W. F. *J. Phys. Chem. B* **2006**, *110*, 25761.
(26) Bougeard, D.; Smirnov, K. S. *Phys. Chem. Chem. Phys.* **2007**, *9*, 226.
(27) Koga, K.; Tanaka, H.; Zeng, X. C. *Nature* **2000**, *408*, 564.
(28) Sen, S. J. *J. Phys. Chem. B* **2002**, 11343.
(29) Levitt, D. G. *Phys. Rev. A* **1973**, *8*, 3050.
(30) Sholl, D. S. *Chem. Phys. Lett.* **1999**, *105*, 269.
(31) Kumar, P.; Buldyrev, S. V.; Starr, F. W.; Giovanbattista, N.; Stanley, H. E. *Phys. Rev. E* **2005**, *72*, 051503.
(32) Bizzarri, A. R.; Cannistraro, S. *Phys. Rev. E* **1996**, *53*, 3040.
(33) Marti, J.; Gordillo, M. C. *J. Chem. Phys.* **2001**, *114*, 10486.
(34) Mamontov, E.; Bumham, C.; Chen, C. J.; Moravsky, A. P.; Loong, C.-K.; de Souza, N. R.; Kolesnikov, A. I. *J. Chem. Phys.* **2006**, *124*, 194703.
(35) Brovchenko, I.; Geiger, A.; Oleinikova, A.; Paschek, D. *Eur. Phys. J. E* **2003**, *12*, 69.
(36) Striolo, A.; Chialvo, A. A.; Gubbins, K. E.; Cummings, P. T. *J. Chem. Phys.* **2005**, *122*, 234712.
(37) Zangi, R. *J. Phys.: Condens. Matter* **2004**, *16*, 5371.
(38) Hirunsit, P.; Balbuena, P. B. *J. Phys. Chem. C* **2007**, *111*, 1709.
(39) Marti, J.; Nagy, G.; Guardia, E.; Gordillo, M. C. *J. Phys. Chem. B* **2006**, *110*, 23987.
(40) Chiessi, E.; Cavalieri, F.; Paradossi, G. *J. Phys. Chem. B* **2005**, *109*, 8091.
(41) Zheng, J.; Lennon, E. M.; Tsao, H.-K.; Sheng, Y.-J.; Jiang, S. *J. Chem. Phys.* **2005**, *122*, 214702.
(42) Bellissent-Funel, M.-C.; Sridi-Dorbez, R.; Bosio, L. *J. Chem. Phys.* **1996**, *104*, 10023.
(43) Berendsen, H. J. C.; van der Spoel, D.; van Drumen, R. *Comput. Phys. Commun.* **1995**, *91*, 43.
(44) Lindhal, E.; Hess, B.; van der Spoel, D. J. *J. Mol. Mod.* **2001**, *7*, 306.
(45) van der Spoel, D. J.; Lindhal, E.; Hess, B.; Groenhof, G.; Mark, A. E.; Berendsen, H. J. C. *J. Comput. Chem.* **2005**, *26*, 1701.
(46) Berendsen, H. J. C.; Postma J. M.; van Gunsteren, W. F.; Hermans, J. In *Intermolecular Forces*; Pullman, B., Ed.; Reidel: Dordrecht, The Netherlands, 1981; pp 331–342.
(47) Bocchinfuso, G.; Stella, L.; Martinelli, S.; Flex, E.; Carta, C.; Pantaloni, F.; Pispisa, B.; Venanzi, M.; Tartaglia, M.; Palleschi, A. *Proteins* **2007**, *66*, 963.
(48) Sheiko, S. S.; Moller, M. *Chem. Rev.* **2001**, *101*, 4099.
(49) Takano, H.; Kenseth, J. R.; Wong, S. S.; O'Brien, J. C.; Porter, M. D. *Chem. Rev.* **1999**, *99*, 2845.
(50) Finot, M. O.; McDermott, M. T. *J. Am. Chem. Soc.* **1997**, *119*, 8564.
(51) Freire, E.; Biltonen, R. L. *Biopolymers* **1978**, *11*, 463.
(52) Barone, G.; Del Vecchio, P.; Fessas, D.; Giancola, C.; Graziano, G. *J. Therm. Anal.* **1992**, *38*, 2779.
(53) Abu-Lail, N. I.; Camesano, T. A. *J. Micron.* **2003**, *212*, 217–238.
(54) Malek, K.; Odijk, T.; Coppens, M.-O. *Nanotechnology* **2005**, *16*, 522.
(55) Berendsen, H. J. C.; Grigera, J. R.; Straatsma, T. P. *J. Phys. Chem.* **1987**, *91*, 6269.
(56) Umemura, M.; Hayashi, S.; Nakagawa, T.; Urakawa, H.; Kajiwara, K. *THEOCHEM* **2003**, *636*, 215.
(57) Umemura, M.; Hayashi, S.; Nakagawa, T.; Urakawa, H.; Kajiwara, K. *THEOCHEM* **2003**, *639*, 69.
(58) Brodka, A. *Mol. Phys.* **1994**, *82*, 1075.
(59) Ohba, T.; Kanoh, H.; Kaneko, K. *Chem. Eur. J.* **2005**, *11*, 4890.
(60) Grisel, M.; Muller, G. *Prog. Colloid Polym. Sci.* **1996**, *102*, 32.

JP076074F